



The solution and diffusion of ruthenium in $\text{UO}_{2\pm x}$

Gerdjan Busker^a, Robin W. Grimes^{a,b,*}, Mark R. Bradford^c

^a Department of Materials, Imperial College, London SW7 2BP, UK

^b Los Alamos National Laboratory, MS K765, Los Alamos, NM 87545, USA

^c British Energy Generation Ltd., Barnwood, Gloucestershire GL4 3RS, UK

Received 20 December 2001; accepted 9 November 2002

Abstract

Atomic scale computer simulation is used to develop models that describe the behaviour of ruthenium in the uranium dioxide lattice. Results are consistent with observed metal particle formation in UO_{2-x} and UO_2 . Conversely it is predicted that ruthenium can be soluble in UO_{2+x} although in irradiated fuel the extent of ruthenium solution will depend on the total concentration of fission products compared to the oxygen interstitial ion concentration. Second phase oxide particles such as BaRuO_3 and RuO_2 are not predicted to be stable. At all stoichiometries activation energies for migration are high.

© 2003 Elsevier Science B.V. All rights reserved.

1. Introduction

In highly irradiated uranium dioxide fuel the noble metal fission products Ru, Rh, Pd, Tc and Mo form a separate metallic phase [1–3]. This usually takes the form of small dispersed grains, referred to as five-metal particles. These exhibit the hexagonal ϵ -Ru crystal structure although at lower burn-up the major constituent element is generally Mo. The particles have been observed within fission gas bubbles at grain boundaries and at inter-granular positions. Presumably the metal atoms must migrate through the lattice to reach the grain boundaries or bubbles, although the atomic scale mechanisms are not known.

In the event of a fault, which results in exposure of hot fuel to an oxidising atmosphere, progressive oxidation of $\text{UO}_2 \rightarrow \text{UO}_{2+x} \rightarrow \text{U}_4\text{O}_9 \rightarrow \text{U}_3\text{O}_{8-z}$ will occur, with the stable phase being determined by the atmosphere and temperature [2,4–6]. If the atmosphere is sufficiently oxidising, then ruthenium will also be ox-

idised forming RuO_3 and RuO_4 , both of which are highly volatile [7–9]. This facilitates the release [9] of Ru-106, which has a half-life of 1.01 years. Although it is clear that ruthenium is quite mobile along grain boundaries [10], the relative mobility in grain interiors has not been established unequivocally [7]. To what extent the transport of ruthenium occurs during the oxidation to UO_{2+x} or only once U_3O_{8-z} is formed [6] is therefore not clear. However, recent work [11,12] does show that oxygen content and oxidation are important in enhancing or reducing ruthenium release. Significantly, established Ellingham diagrams [2,4] show that the oxygen potential at which Ru oxidises to RuO_2 is marginally above the oxygen potential at which U_3O_8 is formed from UO_{2+x} [13]. Thus RuO_2 should not form on the surface of UO_{2+x} until after U_3O_8 has started to form.

Here we report for UO_{2-x} , UO_2 and UO_{2+x} solution energies of ruthenium in a variety of charge states. Seven possible trap sites are considered including simple substitution at a uranium site, substitution at complex vacancy clusters and interstitial solution. These data are then used to determine the starting point for migration activation energy predictions. In all cases, energies associated with ruthenium ions are calculated using atomic scale computer simulation based on inter-ionic potentials and energy minimisation.

* Corresponding author. Tel.: +44-207 594 6730; fax: +44-207 594 6729/584 3194.

E-mail address: r.grimes@ic.ac.uk (R.W. Grimes).

2. Methodology

2.1. The perfect lattice

The atomic scale computer simulation techniques used here are based on energy minimisation with a Born-like description of the lattice [14]. The interactions between ions are composed of two terms: long-range coulombic forces, which are summed using Ewald's method [15], and short-range forces, which are modelled using parameterised pair potentials. The perfect lattice is described by defining a unit cell, which is repeated throughout space using periodic boundary conditions as defined by the usual crystallographic lattice vectors. The lattice energy is then given by:

$$U_L = \frac{1}{4\pi\epsilon_0} \sum_{i \neq j} \frac{q_i q_j}{r_{ij}} + A e^{-r_{ij}/\rho} - \frac{C}{r_{ij}^6} \quad (1)$$

where A , ρ and C are the adjustable parameters specific to ions i and j , r_{ij} is the inter-ionic separation and q is the charge on the ion. The adjustable parameters that describe the U^{4+} – U^{4+} , U^{4+} – O^{2-} and O^{2-} – O^{2-} interactions were taken from previous work [16]. These parameters were derived by fitting to experimental structures and dielectric constants. Parameters that describe the interaction of the various charge states of ruthenium with oxygen and uranium are presented in Table 1 (note: for interactions involving ruthenium the C parameter is zero). These were calculated using the electron gas method [17] since appropriate structures were not available. The exception to this is the Ru^{4+} – O^{2-} potential since data for the RuO_2 lattice (space group $P4_2/mnm$) are available. A small modification to the electron gas potential resulted (although the conclusions did not alter). The resulting predicted lattice parameters for RuO_2 ($a = 0.4510$ nm, $c = 0.3107$ nm) are in excellent agreement with experiment ($a = 0.44968$ nm, $c = 0.31049$ nm) [18].

Table 1
Short range potential parameters relating to Eq. (1)

Species	Adjustable parameters	
	A (eV)	ρ (nm)
Ru^0 – U^{4+}	1573.53	0.044653
Ru^0 – O^{2-}	3173.56	0.026770
Ru^+ – U^{4+}	2851.20	0.037310
Ru^+ – O^{2-}	2603.30	0.029410
Ru^{2+} – U^{4+}	6121.46	0.031310
Ru^{2+} – O^{2-}	2649.29	0.030238
Ru^{3+} – U^{4+}	11 117.43	0.027846
Ru^{3+} – O^{2-}	2988.58	0.029821
Ru^{4+} – U^{4+}	17717.22	0.025595
Ru^{4+} – O^{2-}	3080.00	0.029072

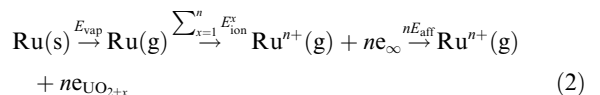
The electronic polarisability of ions is accounted for via the shell model of Dick and Overhauser [19]. This model consists of a massless shell with charge, $Y|e|$, that is allowed to move with respect to a massive core of charge, $X|e|$; therefore, the overall charge state of each ion I is equal to $(X + Y)|e|$. The core and shell charges are connected by an isotropic harmonic spring of force constant k . In all calculations, O^{2-} and U^{4+} are treated as polarisable. For O^{2-} , $Y = -4.04$, $k = 29 680$ eV nm $^{-2}$; for U^{4+} , $Y = 6.54$, $k = 9824$ eV nm $^{-2}$; for Ru^{4+} , $Y = -1.00$, $k = 3500$ eV nm $^{-2}$.

2.2. The defective lattice

Since ruthenium ions may exhibit charge states that are different to those of ions normally at lattice sites in UO_2 and they are usually of a different size, an approach is needed that is able to model the effect of such defects on the surrounding lattice ions. In other words, the calculations of defect energies must include the resulting structural relaxation or displacement polarisation. This is achieved by partitioning the energy-minimised perfect lattice into three concentric spherical regions [20]. In region I, ions are treated explicitly and relaxed to zero strain. The defect is positioned near the centre of this region. Region IIa is an interfacial region where forces between ions are determined via the Mott–Littleton approximation [21], and these ions are relaxed to zero strain. The interaction energies between ions in region IIa and region I are calculated explicitly. The outer region IIb extends to infinity and provides the Madelung field of the remaining crystal. The relaxation energy of ions in region IIb is determined using the Mott–Littleton approximation [21].

2.3. Solution energy calculations

Solution of ruthenium will be determined with reference to the metal since we wish to predict when the metal particles are soluble in the fuel matrix. If ruthenium is soluble, it would be dispersed in the fuel at an atomic level. Thus the first term in calculating the internal energy of solution is the enthalpy of vapourisation of ruthenium metal; $E_{\text{vap}} = 6.72$ eV per metal atom [22] (see step one in Eq. (2)).



Once in the fuel, a ruthenium ion will assume a charge state that minimises the total energy. Thus the ruthenium atom $Ru(g)$ is first ionised to form the appropriate gas phase ruthenium ion $Ru^{n+}(g)$. The total energy for the ionization of isolated ruthenium atom [23], $\sum E_{\text{ion}}^x$ (where $x = 1\text{st}, 2\text{nd}$ etc.), must also be included in the

energy balance (step 2 in Eq. (2)). Each of the resulting n electrons, ne , occupy states in the host fuel. This term, the electron affinity of the fuel, E_{aff} , depends on the stoichiometry of the fuel. Following previous calculations [16], in UO_{2-x} this is zero, in UO_{2+x} , $E_{\text{aff}} = 2.3$ eV (the band gap energy) and in UO_2 , $E_{\text{aff}} = 1.15$ eV (half the band gap energy).

It is then necessary to calculate the energy gained or lost by incorporating the resulting ruthenium ion, Ru^{n+} , in a pre-existing trap site in the fuel lattice. This energy, (the incorporation energy [16]), does not depend on stoichiometry since the trap site is pre-existing, however the energy required or released varies greatly between trap sites. Finally, it is necessary to calculate the energy to form the trap site that is to be occupied. The reason such a term must be included is that we assume the number of ruthenium ions available for solution is significantly higher than the number of available trap sites (which are minority defects). This is justified because such trap sites have concentrations typically orders of magnitude less than the level of non-stoichiometry. These internal energies for trap site formation have a strong dependence on stoichiometry. The defect equations that govern these terms are a consequence of the equilibrium established between the trap site formation and the majority oxygen Frenkel defect reaction and have been described in detail previously [16]. Thus we implicitly assume that the total concentration of fission product ions is less than the level of the majority defects (e.g. from non-stoichiometry). We shall return to this point later.

2.4. Migration calculations

Activated migration mechanisms consist of sequential jumps of the migrating ion either between vacant lattice sites or between interstitial sites. The activation energy for the migration process, once the defects are in registry, is the difference between the energy of the system when the migrating ion is at the saddle point and the energy of the ion in the trap site adjacent to the defect that mediates the migration mechanism. Here the saddle point energy is calculated by introducing a fixed ruthenium ion at the saddle point location and then relaxing the surrounding lattice. Evaluating the potential energy surface both parallel and perpendicular to the diffusion path identifies the configuration of the saddle point.

For example, if the ruthenium ion occupies a simple uranium vacancy site, a second uranium vacancy is required to mediate the migration process. In such circumstances, the migration energy is the sum of the energy to associate the mediating uranium vacancy to the ruthenium trap site plus the energy for the hopping process. However, it may be that the activation energy necessary for the uranium vacancy to migrate through the lattice to the trap site is a higher energy process. In

such circumstances, this is what will be measured experimentally. Such cation self-diffusion in UO_2 has not been calculated, but taken from experiment. Matzke [24] reports Arrhenius energies of 5.0–7.8 eV for UO_{2-x} , 5.6 eV for UO_2 and 2.6 eV for UO_{2+x} .

Finally, the trap site may be a complex defect cluster. Although this makes the saddle point identification more difficult, the same process is employed to find the saddle point. Furthermore migration and association or dissociation of a uranium vacancy or cluster fragment (if the solution site is large) is still necessary.

3. Results

3.1. Solution with respect to metal particles

The internal energies for ruthenium metal solution are presented in Table 2. Five charge states are considered and solution is determined with respect to an isolated uranium vacancy (Ru_{U}), an isolated oxygen vacancy (Ru_{O}), a di-vacancy consisting of an adjacent uranium and oxygen vacancy pair (Ru_{UO}), four other different defect vacancy clusters and the interstitial site. In previous studies [16], atoms such as Xe and Cs have shown preference for the neutral tri-vacancy (i.e. Xe_{UO_2}). Here solution is favoured in similar sites: in UO_{2-x} , as Ru^{2+} in either a di-vacancy or a neutral tri-vacancy, in UO_2 as Ru^{2+} or Ru^{3+} but exclusively substituted in a uranium vacancy and in UO_{2+x} as Ru^{3+} in a uranium vacancy (although in UO_{2+x} solution is possible in a di-uranium vacancy). Thus the highest predicted charge state is Ru^{3+} and not Ru^{4+} . In our model this reflects the value of the fourth ionization energy of ruthenium [23] (47.96 eV) compared to uranium [25] (31.06 eV): the magnitude of the electrostatic or Madelung field in UO_2 is simply not sufficient to promote the fourth ionization of ruthenium (in fact even the fifth ionization energy of uranium is predicted to be only 45.77 eV [25]). The result also seems sensible in the light of the experimentally observed position of the Ru/ RuO_2 oxygen potential relative to that of $\text{UO}_2/\text{U}_3\text{O}_8$ [2,13].

By considering the sign and magnitude of the solution energies in Table 2, it is also clear that solution in UO_{2-x} and UO_2 is not favoured with respect to the metal, in agreement with the observed formation of ϵ -Ru particles. However, solution is favoured in UO_{2+x} . Thus we predict that no ruthenium will be lost from the fuel to metal particles under strongly oxidising conditions. Indeed on this basis alone, given the magnitude of the negative solution energy in UO_{2+x} it is feasible that at least the ruthenium portion of the metal particles will begin to undergo resolution.

We should now return to the point made at the end of Section 2.3 concerning the concentration of fission products compared to the level of hyper-stoichiometry.

Table 2
Solution energies (eV) of ruthenium ions, Ruⁿ, into UO_{2±x} relative to ruthenium metal

Solution site	Ru ⁰	Ru ⁺	Ru ²⁺	Ru ³⁺	Ru ⁴⁺
<i>UO_{2-x}</i>					
Interstitial	24.95	18.92	18.12	20.71	26.81
Ru _U	24.38	17.35	14.84	15.85	23.06
Ru _{UO}	20.88	15.01	13.41	14.99	21.81
Ru _{UO₂}	18.80	14.34	13.79	16.09	22.88
Ru _{U₂}	42.29	34.11	30.41	30.27	36.18
Ru _{U₂O}	34.58	27.84	25.32	26.00	31.88
Ru _{U₂O₂}	27.67	22.67	21.45	23.15	29.43
Ru _O	22.81	19.66	21.04	24.94	30.99
<i>UO₂</i>					
Interstitial	24.95	17.77	15.82	17.26	22.21
Ru _U	17.57	9.39	5.73	5.59	11.65
Ru _{UO}	17.48	10.45	7.71	8.14	13.81
Ru _{UO₂}	18.80	13.19	11.49	12.64	18.28
Ru _{U₂}	28.67	19.34	14.49	13.20	17.97
Ru _{U₂O}	24.37	16.48	12.81	12.33	17.06
Ru _{U₂O₂}	20.86	14.72	12.35	12.89	18.02
Ru _O	26.21	21.92	22.15	24.90	29.79
<i>UO_{2+x}</i>					
Interstitial	24.95	16.62	13.52	13.81	17.61
Ru _U	10.76	1.44	-3.37	-4.66	0.24
Ru _{UO}	14.07	5.90	2.01	1.28	5.81
Ru _{UO₂}	18.80	12.04	9.19	9.19	13.68
Ru _{U₂}	15.06	4.60	-1.42	-3.86	-0.25
Ru _{U₂O}	14.16	5.12	0.30	-1.33	2.25
Ru _{U₂O₂}	14.05	6.76	3.24	2.63	6.61
Ru _O	29.61	24.17	23.25	24.85	28.60

Negative energies imply solubility.

The problem is that for higher burn-up fuels, the total concentration of fission products including ruthenium may be higher than that of the oxygen interstitial ions required to compensate the solution process. In such circumstances the equilibria between solution mechanisms for various fission products (e.g. Mo, Ce and rare earth elements in addition to Ru) will lead to a certain fraction of these elements precipitating into either metal particles or gray phase oxide particles. Consequently we envisage that a partition will be established so that a proportion of the ruthenium (and other five metal particle elements) will be in the form of metal particles even in nominally UO_{2+x}. The amount of the ruthenium in the metal particles will be a function of burn-up, hyperstoichiometry and operating temperature. This should be taken into consideration when interpreting experimental data.

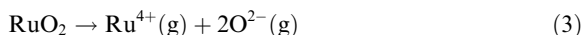
3.2. Solution with respect to a secondary oxide phase

Although metal particles may be soluble in UO_{2+x} it is possible given the elevated oxygen partial pressure that the available ruthenium is incorporated into a secondary oxide phase different than that of the fuel matrix.

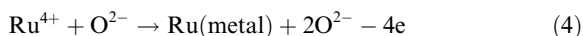
For example, many fission products are incorporated into grey phase particles [2] that are essentially substituted barium zirconate perovskite. Thus a representative second oxide phase to consider would be BaRuO₃ perovskite (although BaRuO₃ is not expected to form as a single phase). Although RuO₂ should not form, as discussed in the introduction [2,4,13], we will consider formation of RuO₂ as a test of the predictive capability of our method. (Note: although we predict that Ru⁴⁺ will not form in UO_{2±x} this does not mean that in another oxide with a higher Madelung field ruthenium will not assume a 4+ charge state.) As stated previously, RuO₂ has the rutile structure [18] and is very well reproduced by these potentials. BaRuO₃ exhibits a nine layer rhombohedral structure (9R) related to perovskite [26], rather than a simple cubic perovskite. We correctly predict the rhombohedral structure to be lower in energy than the cubic polymorph and a negative reaction enthalpy when RuO₂ and BaO form BaRuO₃ ($\Delta E = -0.69$ eV).

The problem of calculating the solution energies for RuO₂ in UO_{2±x} is simplified by noting that it is possible to determine the difference in solution energy between dissolving metal and oxide. These different energies can

then be added to the values in Table 2 to yield solution energies for the oxide. The differences stem from the fact that RuO_2 can be dissociated and accommodated via the following reactions. First,



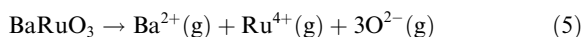
This requires the lattice energy, that is, -120.37 eV for RuO_2 per formula unit (for BaRuO_3 the energy is -152.82 eV). Second,



The energy to remove four electrons (4e) from the lattice was described in Section 2.3. Finally, the oxygen ions are accommodated in the lattice, in equilibrium with the Frenkel reaction. This is therefore a function of stoichiometry and in UO_{2-x} , the oxygen ions will occupy oxygen vacancies (contributing -33.04 eV), in UO_{2+x} , the oxygen ions occupy interstitial sites (contributing -19.42 eV) and in UO_2 , they are shared equally between interstitial and vacancy sites (contributing -26.23 eV). The total difference terms between solution of oxide and metal are therefore: -21.07 eV for UO_{2-x} , -9.67 eV for UO_2 and 1.74 eV for UO_{2+x} . The total solution energies for RuO_2 are therefore -7.66 eV in the UO_{2-x} lattice, -4.08 eV in UO_2 and -2.92 eV in UO_{2+x} . Clearly, RuO_2 is always predicted to be soluble in uranium dioxide irrespective of stoichiometry.

At this point it is interesting to compare the present solution energies for RuO_2 with those of ZrO_2 which are small but slightly positive [16] or with CeO_2 which is also small and positive in UO_{2-x} and UO_2 but slightly negative for UO_{2+x} [16]. The reason that RuO_2 behaves so differently is that ruthenium is readily able to assume lower charge states and it is this additional contribution to the solution energy that results in its high solubility. Of course, if any RuO_2 were present our energies indicate that it would transfer oxygen to the fuel lattice leaving ruthenium metal. This prediction is fully consistent with available thermodynamic data [6].

The possible solubility of BaRuO_3 can now also be addressed. In this case Eq. (3) is modified so that Ba^{2+} ions are formed which must also be accommodated in the lattice.



Previous calculations [16] of Ba^{2+} solution have been repeated here with the larger simulation sizes now available but the results remain very similar giving energies of: -11.55 eV in UO_{2-x} , -16.91 eV in UO_2 and -23.71 eV in UO_{2+x} . Using these values together with values for solution of ruthenium (above) and modified energies for accommodation of the additional oxygen, yields solution energies for BaRuO_3 of: -6.83 eV in UO_{2-x} , -1.87 eV in UO_2 and -4.02 eV in UO_{2+x} . Clearly

the possibility of forming this specific more complex oxide does not change the predicted preference for ruthenium accommodation as stated previously. That is, BaRuO_3 is not thermodynamically stable compared to either the metal (in the cases of UO_{2-x} and UO_2) or ruthenium ions dissolved in the fuel matrix (in the case of UO_{2+x}). This is consistent with the lack of reported observations of BaRuO_3 as a secondary phase. The extent to which BaRuO_3 is a representative model for the gray phase is debatable but we also note that solution of Ru in the gray phase has also not been reported.

3.3. Ruthenium ion migration energies

As described in Section 2.4, the calculated migration activation energy for ruthenium will depend on the equilibrium site of the ruthenium atom or ion. However, since we predict that ruthenium never occupies the interstitial site, in all cases it is necessary to associate additional vacancies with the trap site or dissociate vacancies from the trap site.

Table 2 shows that in UO_{2+x} the equilibrium trap site is a uranium vacancy and that the charge state is $3+$. The equilibrium energy to associate a second uranium vacancy is only 0.80 eV. Again this value can be determined from Table 2 since it is the difference between the Ru^{3+} solution energies in Ru_U and Ru_{U_2} . The calculated energy for a Ru^{3+} ion to migrate between the two uranium sites in this U_2 cluster is 6.12 eV. The total migration energy is therefore 6.92 eV. Transport of ruthenium via the U_2 cluster constitutes the lowest predicted migration pathway in UO_{2+x} . However it is considerably higher than the experimental activation energy [24] for uranium migration (which is 2.6 eV). Consequently uranium vacancy migration is not the rate determining process for the transport of ruthenium. A similar conclusion has been reached for iodine and caesium migration in UO_{2+x} although activation energies in this case were much smaller [27]. Further details and all predicted energies for migration can be found in Ref. [28].

In UO_2 , Table 2 shows that the equilibrium trap site is again a uranium vacancy, although the charge state is somewhat ambiguous being potentially either $2+$ or $3+$. Furthermore, these simulations predict that the lowest energy trap site for migration process will be a U_2O_2 vacancy cluster. This is mostly due to the lower energy difference between Ru_U and $\text{Ru}_{\text{U}_2\text{O}_2}$ (for either Ru^{2+} or Ru^{3+}) compared to the difference between Ru_U and Ru_{U_2} (see Table 2). However, the migration activation energy within the U_2O_2 trap is 4.61 eV for Ru^{2+} but substantially higher at 6.20 eV for Ru^{3+} . Consequently, the lowest migration energy, 11.37 eV, is for Ru^{2+} . Again this energy is substantially higher than that for uranium vacancy migration. This conclusion contrasts

with that for iodine and caesium in UO_2 where uranium vacancy migration is the rate determining step [27].

Finally, for UO_{2-x} a different mechanism will operate. Table 2 shows that the equilibrium trap is for Ru^{2+} in either a di-vacancy Ru_{UO} or neutral tri-vacancy Ru_{UO_2} . However, the energy to associate another uranium vacancy or larger fragment is very high (Table 2 suggests close to 10 eV). The energy for the ruthenium ion to hop within such a larger cluster is then over 4 eV so that the overall energy would be in excess of 14 eV. Alternatively, the di-vacancy may dissociate to leave a Ru^+ ion in an oxygen vacancy. Although the energy for that process is also high ($19.66 - 13.41 = 6.25$ eV), the energy for the ruthenium ion to move within the small di-vacancy is practically zero so that the migration energy remains 6.25 eV. In this case, the migration energy is similar to that for uranium vacancy migration (5.0–7.8 eV [24]).

At all stoichiometries these predicted activation energies for ruthenium migration through the lattice, which assume formation of traps under equilibrium conditions, are high. Consequently equilibrium resolution of metal particles into UO_{2+x} will be greatly limited. Furthermore it seems likely that migration of ruthenium to the metal particles will require radiation enhanced transport.

4. Discussion and conclusions

The solution energy predictions presented here are consistent with the experimental observations that ruthenium forms metal particle precipitates in UO_{2-x} and UO_2 . In UO_{2+x} , ruthenium is predicted to be soluble only up to the point where there are sufficient oxygen interstitial ions to compensate the solution mechanism. Therefore ruthenium may still be observed in metal particles so long as the value of x is appropriately small. Significantly, high temperature experiments in air describe ruthenium loss from UO_{2+x} using a $1 - \exp(-kt)$ release rate model [29]. This is analogous to surface controlled evaporation from a solution and is based on the assumption that the rate of release is proportional to the remnant fraction with mass transfer control depending on the vapour pressure above the surface. The release rate is then proportional to the saturated vapour pressure times the thermodynamic activity. For an ideal solution the activity is equal to the mole fraction. Our prediction that ruthenium is soluble in UO_{2+x} is entirely consistent with such a model.

However, there are a number of steps involved in the loss of ruthenium from the surface. In the bulk, we predict the charge state of ruthenium to be 3+ (or possibly 2+). At the surface ruthenium is removed by forming RuO_3 and RuO_4 vapour above RuO_2 . Ruthenium must therefore undergo oxidation at or near to the surface. Thermodynamic data show that this will not

occur until the oxygen potential is sufficient that UO_{2+x} is being oxidised to U_3O_8 [2,4,13]. The rate-determining step for the loss of ruthenium from the UO_{2+x} lattice is thus not clear. It could be:

- the activation energy for ruthenium migration through the lattice (quite possible given the high predicted values)
- a segregation barrier at the surface
- the surface oxidation of ruthenium to form RuO_2 (which may or may not reflect the bulk equilibrium situation)
- further oxidation to form RuO_3 and RuO_4 vapour or
- mass transport from the surface.

Of course, if sufficient oxygen is not available, this itself will be a critical limiting factor for ruthenium loss, at least via vapour transport [9].

Acknowledgements

This report and the work it describes was funded by the Health and Safety Executive. Its contents, including any opinions and/or conclusions expressed, are those of the authors alone and do not necessarily reflect HSE policy. Computing facilities were provided through EPSRC grant GR/M94427. RWG gratefully acknowledges Los Alamos National Laboratory for support through the Bernd T. Mattias Scholarship. The authors would like to thank Dr John Evans for informative discussions.

References

- [1] F.T. Ewart, R.G. Taylor, J.M. Horspool, G. James, J. Nucl. Mater. 61 (1976) 254.
- [2] H. Kleykamp, J. Nucl. Mater. 131 (1985) 221.
- [3] L.E. Thomas, R.E. Einziger, R.E. Wooley, J. Nucl. Mater. 166 (1989) 243.
- [4] M.R. Bradford, Nucl. Energy 35 (1996) 321.
- [5] R.R. Hobbins, D.J. Osetek, D.A. Petti, D.L. Hagerman, in: J.T. Rogers (Ed.), Fission product transport processes in reactor accidents, Hemisphere, 1990, p. 215.
- [6] R. Williamson, S.A. Beetham, in: J.T. Rogers (Ed.), Fission product transport processes in reactor accidents, Hemisphere, 1990, p. 175.
- [7] M.A. Mansouri, D.R. Olander, J. Nucl. Mater. 254 (1998) 22.
- [8] E.H.P. Cordfunke, R.J.M. Konings, Thermochemical data for reactor materials and fission products, North Holland Science Publications, 1990, Tables A109 and A121–126.
- [9] F.C. Iglesias, C.E.L. Hunt, F. Garisto, D.S. Cox, in: J.T. Rogers (Ed.), Fission product transport processes in reactor accidents, Hemisphere, 1990, p. 187.
- [10] D.R. Olander, Nucl. Sci. Eng. 82 (1982) 190.

- [11] C. Ronneau, J. Cara, A. Rimski-Korsakov, *J. Environ. Radioactivity* 26 (1995) 63.
- [12] P. Froment, J. Cara, J. Vanbegin, C. Ronneau, *Radiochim. Acta* 89 (2001) 155.
- [13] Y.S. Kim, *J. Nucl. Mater.* 279 (2000) 173.
- [14] M. Born, *Atomtheorie des festen Zustandes*, Teubner, Leipzig, Germany, 1923.
- [15] P.P. Ewald, *Ann. Phys. (Leipzig)* 64 (1921) 253.
- [16] R.W. Grimes, C.R.A. Catlow, *Phil. Trans. R. Soc. Lond. A* 335 (1991) 609.
- [17] J.H. Harding, A.H. Harker, Harwell Laboratory, Technical Report AERE – R 10425, 1982.
- [18] A.A. Bolzan, C. Fong, B.J. Kennedy, C.J. Howard, *Acta Cryst. B* 53 (1997) 373.
- [19] B.G. Dick, A.W. Overhauser, *Phys. Rev.* 112 (1958) 90.
- [20] C.R.A. Catlow, W.C. Mackrodt (Eds.), *Computer simulation of solids*, Springer-Verlag, Berlin, Germany, 1982.
- [21] N.F. Mott, M.J. Littleton, *Trans. Faraday Soc.* 34 (1932) 485.
- [22] L. Brewer, G.M. Rosenblatt, *Adv. High Temp. Chem.* 2 (1969) 1.
- [23] D.R. Lide (Ed.), *CRC handbook of chemistry and physics*, 78th ed., CRC, Boca Raton, FL, 1997–1998.
- [24] H.J. Matzke, in: E. J. Hastings (Ed.), *Advances in ceramics*, vol. 17, Am. Ceram. Soc., 1986, p. 1.
- [25] N.C. Pyper, I.P. Grant, *J. Chem. Soc. Faraday Trans.* 74 (1978) 1885.
- [26] P.C. Donohue, L. Katz, R. Ward, *Inorg. Chem.* 4 (1965) 306.
- [27] G. Busker, R.W. Grimes, M.R. Bradford, *J. Nucl. Mater.* 279 (2000) 46.
- [28] G. Busker, PhD thesis, University of London, 2002.
- [29] J.L. Kelly, A.B. Reynolds, M.E. McGown, *Nucl. Sci. Eng.* 88 (1984) 184.